JOURNAL OF MATERIALS SCIENCE **34** (1999) 4447–4455

Weibull master curves and fracture toughness testing

Part III *Master curves for the evaluation of dynamic Charpy impact tests*

M. LAMBRIGGER
Centre de recherches en physique des plasmas, Technologie de la Fusion, EPFL, Im Struppen 12, CH 8048 Zürich, Switzerland

The existence of specimen-size-independent quasi-static Weibull master curves for macroscopically homogeneous solids characterizing strength and failure of both purely brittle materials and rather tough materials, which undergo an amount of stable crack growth prior to failure, has already been proved in earlier publications. In this paper, the concept of Weibull master curves is extended to the case of dynamic testing conditions, being typical for Charpy impact tests performed in the ductile-to-brittle transition temperature-range of ferritic-martensitic steels. Dynamic Weibull master curves can be constructed, if the stress-distributions, which are built up in the process zone of the specimens during the Charpy impact tests, can be described with a dynamic quasi-equilibrium approach. In this case, the dynamic Weibull master curves can be related to the quasi-static Weibull master curves with the help of the toughening exponent τ, characterizing the rate of toughness increase with increasing crack length. Characteristic magnitudes, being most convenient to estimate the capacity of the tested materials to undergo stable crack growth, microcracking and crack-tip shielding prior to rupture, can be derived as well from dynamic Weibull master curves as from quasi-static Weibull master curves.

Nomenclature

v_{pend}	pendulum velocity at begin of impact
d_i, β	constants
c	crack length
r	numerical constant characterizing the geometry of the localized loading
σ	applied failure stress or normal stress built up in the process zone
$\sigma_{\max}$	maximum normal stress
$P(\sigma)$	quasi-static, three-parameter, cumulative Weibull failure probability distribution function
σ_0	normalizing factor in dimensions of stress
σ_τ	threshold stress, below which no failure occurs
σ_{in}	failure stress at the inflexion point of $P(\sigma)$
$\bar{\sigma}$	mean failure stress
m	Weibull modulus
z	distinct value of the cumulative failure probability distribution function
σ_z	failure stress corresponding to the cumulative failure probability z
K_I	failure stress intensity
τ	toughening exponent
R	work necessary for incremental crack extension
T	fracture resistance
E	Young's modulus
P	pendulum force acting on the Charpy specimen
F	localized load
P'	reaction line-force built up at the notch-tip of the Charpy specimens during testing
K_{a}	separated stress intensity factor due to uniform applied stress
K_{r}	separated stress intensity factor due to localized, residual stress field
m'	dynamic Weibull modulus
$P_{\max}$	maximum impact line-force built up during the Charpy impact test

$P(P_{\max})$	dynamic, two-parameter, cumulative Weibull failure probability distribution function
$P'_{\max}$	maximum reaction line-force at the notch-tip arising during the Charpy impact test
$P_{\max 0}$	normalizing factor in dimensions of load
$P_{\max \tau}$	threshold load-value
$P_{\max z}$	maximum impact line-force corresponding to the cumulative failure probability z
$P_{\max in}$	maximum impact line-force at the inflexion point of the two-parameter, cumulative Weibull failure probability distribution function $P(P_{\max})$
$\bar{P}_{\max}$	mean-value of the maximum impact line force
σ_f, F_f, c_f	values of σ, F and c corresponding to the onset of unstable crack propagation
$I(x, m)$, $K(y, m)$ and $M[e(z), m]$	three different types of quasi-static, theoretical Weibull master curves
$I\exp(x, m)$, $K\exp(y, m)$ and $M\exp[e(z), m]$	three different types of quasi-static, experimental Weibull master curves
x, y and $e(z)$	different types of scaled failure stresses
x_{cr}, y_{cr}, $e_{cr}(z)$	values of the cross-over points formed by the corresponding experimental and theoretical master curves
$H[e(z)]$	step function being equal to zero for $e(z) < e_{cr}(z)$ and equal to one for $e(z) \geq e_{cr}(z)$
$FiM1[e(z)]$, $FiM2[e(z)]$, $F\exp 1M[e(z)]$, $F\exp 2M[e(z)]$, χ_M, χ_I and χ_k	deviation parameters derived from the step function $H[e(z)]$ and from the quasi-static Weibull master curves $M[e(z), m]$ and $M\exp[e(z), m]$
$I(x', m')$, $K(y', m')$ and $M[e'(z), m']$	three different types of dynamic, theoretical Weibull master curves
$I\exp(x', m')$, $K\exp(y', m')$ and $M\exp[e'(z), m']$	three different types of dynamic, experimental Weibull master curves
x', $y'$and $e'(z)$	different types of scaled maximum impact line-forces
x'_{cr}, y'_{cr}, $e'_{cr}(z)$	values of the cross-over points formed by the corresponding experimental and theoretical master curves
$H'[e'(z)]$	step function being equal to one for $e'(z) < e'_{cr}(z)$ and equal to zero for $e'(z) \geq e'_{cr}(z)$
$FiM1'[e'(z)]$, $FiM2'[e'(z)]$, $F\exp 1M'[e'(z)]$, $F\exp 2M'[e'(z)]$, $d\chi_M$, $d\chi_I$ and $d\chi_k$	deviation parameters derived from the step function $H'[e'(z)]$ and from the dynamic Weibull master curves $M[e'(z), m']$ and $M\exp[e'(z), m']$

1. Introduction

9–12 wt % Cr ferritic-martensitic steels with fine carbide structures are considered to be promising applicants for structural materials in fusion technology, mainly because of their high strength, low thermal dilatation and high resistance to void swelling [1]. However, they are sensitive to irradiation embrittlement causing a shift of the ductile-to-brittle transition temperature (DBTT) to higher values [2]. The DBTT is generally studied with the help of instrumented Charpy impact tests [3], which are performed at distinct testing-temperatures. These tests provide the Charpy energies (absorbed impact energies) of the specimens, being evaluated by integration of the measured load versus time diagrams [3]. Charpy energy versus temperature diagrams are generally used in order to characterize the ductile-to-brittle transition of ferritic-martensitic steels.

In this paper, the scatter of the maximum pendulum force for a definite material at a fixed testing-temperature in the DBTT-range, is studied by performing series of instrumented Charpy impact tests. Therefore, the quasi-static Weibull model has been modified into a dynamic Weibull model, which is applicable to uniaxial, localized dynamic loading conditions. The quasi-static and the dynamic Weibull models enable qualification and quantification of the amount of microcrack-nucleation, microcrack-propagation, crack-tip shielding and stable crack growth having been undergone by the tested samples prior to rupture, by simply testing 20 to 30 specimens under equal testing-conditions. Nucleation and stable growth of (micro-)cracks are supposed to be important parameters in estimating DBTT-shifts due to irradiation embrittlement.

In part 1 and 2 of this series of papers [4, 5], the specimen-size-independent, three-parameter cumulative failure probability distribution function $P(\sigma)$ has been shown as significant, if an uniaxial tensile stress σ is applied to the investigated specimens under quasi-static loading conditions, as for example in tensile or bend tests. Specimen-size-independent Weibull master curves represent scaled cumulative failure probability distribution functions. The general type of Weibull master curves $M[e(z), m]$ is obtained by scaling $P(\sigma)$ with any stress σ_z corresponding to a distinct, cumulative failure probability z. As a result, the following transformations can be performed [4],

$$P(\sigma) = 1 - \exp\left\{-\left(\frac{\sigma - \sigma_\tau}{\sigma_0}\right)^m\right\}; \quad \sigma > \sigma_\tau \qquad (1)$$

$$P(\sigma_z) = z \qquad (2)$$

whereby m denotes the Weibull modulus, σ_τ the threshold failure stress underneath $P(\sigma)$ is zero and σ_0 a

normalizing factor which has dimensions of stress. If the variable transformation

$$e(z) = \frac{\sigma - \sigma_\tau}{\sigma_z - \sigma_\tau} \tag{3}$$

has been accomplished, the quasi-static Weibull master curves $M[e(z), m]$ are obtained [4]:

$$P(\sigma) = M[e(z), m] = 1 - (1 - z)^{[e(z)]^m} \tag{4}$$

Two further types of quasi-static Weibull master curves $I(x, m)$ and $K(y, m)$, repesenting special cases of $M[e(z), m]$, are calculated by scaling $P(\sigma)$ with the mathematically relevant stress-value of the corresponding inflexion point σ_{in} or by scaling $P(\sigma)$ with the physically highly significant mean stress $\bar{\sigma} = \int_0^1 \sigma dP$. $I(x, m)$ exists for $m < 0$ and $m > 1$, whereas $K(y, m)$ always exists for $m < -1$ and $m > 0$. The scaled failure stress x and y are defined as follows [4]:

$$x = \frac{\sigma - \sigma_\tau}{\sigma_{\text{in}} - \sigma_\tau} \tag{5}$$

$$y = \frac{\sigma - \sigma_\tau}{\bar{\sigma} - \sigma_\tau} \tag{6}$$

Thus, the special master curves $I(x, m)$ and $K(y, m)$ can be written as follows;

$$P(\sigma) = I(x, m) = 1 - \exp\left[\frac{(1 - m)}{m} x^m\right] \tag{7}$$

$$P(\sigma) = K(y, m) = 1 - \exp\left\{-\left[\Gamma\left(1 + \frac{1}{m}\right)\right]^m y^m\right\} \tag{8}$$

whereby $\Gamma(1 + \frac{1}{m})$ represents the complete Gamma-function [4].

In part 2 of this series of papers [5], it has been displayed that quasi-static experimental Weibull master curves of materials undergoing an amount of stable crack growth prior to failure, facilitate the characterization of the toughening mechanisms operating in the investigated materials. The quasi-static experimental Weibull master curves are derived from uniaxial tensile or bend tests [5]. Furthermore, it has been shown that the quasi-static experimental Weibull master curves $M \exp[e(z), m]$, $I \exp(x, m)$ and $K \exp(y, m)$ can be constructed with the help of special numerical or graphical techniques, by simply calculating the Weibull modulus m from the upper σ-range of the experimental, cumulative failure stress distributions $P(\sigma_i)$ [4–8]. Besides, $m > 0$ has been verified under quasi-static conditions. In order to evaluate experimental failure data $(\sigma_i, P(\sigma_i))$, a step function $H[e(z)]$ being equal to zero for scaled failure stresses $e(z) < e_{\text{cr}}(z)$ and equal to one for $e(z) \geq e_{\text{cr}}(z)$, has been defined [5]. The two areas formed between $H[e(z)]$ and $M[e(z), m]$ are denoted by $FiM1[e(z)]$ and $FiM2[e(z)]$. $F \exp 1M[e(z)]$ and $F \exp 2M[e(z)]$ represent the two corresponding areas formed between $M[e(z), m]$ and $M \exp[e(z), m]$. $FiM1[e(z)]$ and $F \exp 1M[e(z)]$ denote the areas, which are situated below the cross-over point $e_{\text{cr}}(z)$ of $M[e(z), m]$ and $M \exp[e(z), m]$, whereas the opposite is valid for $FiM2[e(z)]$ and $F \exp 2M[e(z)]$.

$FiM1[e(z)]$, $FiM2[e(z)]$, $F \exp 1M[e(z)]$ and $F \exp 2M[e(z)]$ are significant deviation parameters, distinguishing the toughening potential of the investigated material. They are used to define the specimen-size-independent, material-specific quotients χ_M given by

$$\chi_M = \frac{FiM1[e(z)]/FiM2[e(z)]}{F \exp 1M[e(z)]/F \exp 2M[e(z)]} \tag{9}$$

The χ_M-values of the special master curves $I(x, m)$ and $K(y, m)$, denoted by χ_I and χ_k, can be calculated as follows, whereby z_{in} and $\bar{z}$ have been defined in detail in Ref. [5]:

$$\chi_I = \frac{FiM1[e(z_{\text{in}})]/FiM2[e(z_{\text{in}})]}{F \exp 1M[e(z_{\text{in}})]/F \exp 2M[e(z_{\text{in}})]} \tag{10}$$

$$\chi_k = \frac{FiM1[e(\bar{z})]/FiM2[e(\bar{z})]}{F \exp 1M[e(\bar{z})]/F \exp 2M[e(\bar{z})]} \tag{11}$$

The static quotients χ_M, χ_I and χ_k being defined for positive Weibull moduli m are material-specific in a first approach [5, 7]. χ_M, χ_I and χ_k are positive and finite for $m > 1$. On the other side, χ_I is not defined for $0 < m \leq 1$, although χ_M and χ_k are also positive and finite for $0 < m \leq 1$.

2. Dynamic model for the evaluation of instrumented Charpy impact tests

In this section a dynamic model for the evaluation of instrumented Charpy impact tests is presented. It can always be applied to materials, whose toughness and acoustic wave speeds are similar to those of ferritic steels being tested below or close to the DBTT.

First, a dynamic quasi-equilibrium is defined. In the case of Charpy impact tests, being performed with ferritic-martensitic steels in the DBTT-range, the dynamic quasi-equilibrium is assumed to be achieved in the process zone of the investigated specimens prior to brittle failure, if the specimens overcome a short inertia-affected load stage. The dynamic quasi-equilibrium approach (DQEA) ensures, that the force P of the pendulum, which is acting on the specimen during a Charpy impact test, is nearly a line force, which is steadily increasing with time prior to failure. The pendulum is also assumed to remain in contact with the specimen after having passed the short inertia-affected load stage. Moreover, it is presumed, that during the dynamic quasi-equilibrium stage a reduced reaction line-force P', being proportional to P, is built up opposite to the contact zone along the notch-tip. P' is mainly the result of longitudinal waves, originating in the impact contact zone and expanding straight-forward along the central bar-channel parallel to the mid-plane down to the notch-tip, where they are reflected (see Fig. 1). According to the DQEA the central bar-channel, which

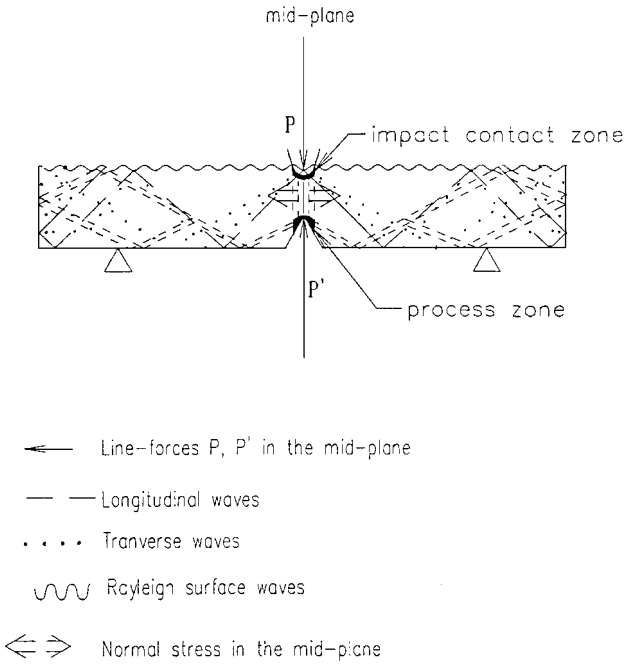

Figure 1 Graph displaying the dynamic quasi-equilibrium approach (DQEA) for Charpy impact testing.

connects the impact contact zone with the process zone, is postulated as the unique relevant transfer zone of these longitudinal waves, which are building up P'. The remaining energy input of the impact line-force P, which is not contributing to the formation of the local reaction line-force P', is assumed as being steadily transformed into Rayleigh surface waves as well as transverse and longitudinal waves, spreading out all over the specimen in all remaining directions. These waves interfere by undergoing (multiple-)reflection and dispersion at grainboundaries and surfaces prior to contributing to the stress distribution in the central bar-channel in an approximately uniform manner. Thus, a relevant, only weakly oscillating normal stress σ is built up in the central bar-channel during the time-interval corresponding to the dynamic quasi-equilibrium, i.e. before final rupture occurs by unstable crack growth (see Fig. 1). On the other side, the axial stress contribution of the multiple-reflected waves is assumed to be negligible in the central bar-channel, if the DQEA can be applied. As a matter of fact, the axial stress component is only relevant with respect to failure mechanisms (such as nucleation and growth of microcracks or cracks, crack-tip shielding etc.) in the small process zone along the notch-tip. Thus, it is evident for physical and geometrical reasons, that the local axial stress contribution of the multiple-reflected waves in the process zone must be very small in comparison to the corresponding local, axial stress contribution of the highly concentrated, longitudinal wave-systems emerging from the impact contact zone and expanding along the central bar-channel down to the notch-tip.

The reaction line-force P' is responsible for the formation of the process zone ahead of the notch-tip. The local strain rate in the process zone is estimated as having values between 10^2 and 10^3 s^{-1}, if usual pendulum velocities (1 m/s $< v_{pend} <$ 5 m/s) and common specimen-geometries are chosen, and if the DQEA can be applied. Thus, the process zones may be formed, in this case, by localized, elasto-plastic deformation under dynamic, partially adiabatic conditions [9]. The arising residual stress field, due to the process zone ahead of the notch-tip, is crucial for the subsequent stable growth of cracks and microcracks, which nucleate from initial defects in the process zone. According to the DQEA only the normal stress σ is significant in the process zone close to the notch-tip in addition to the local reaction line-force P'. Therefore, it has already implicitly been stated that for the analysis of the time-interval, which is characterized by both the passage of the maximum impact line-force P and the stable growth of the critical crack giving rise to final rupture, only the approximately uniform normal stress σ and P' need to be considered.

Moreover, it may be assumed, that an increase of the pendulum force P by a factor β goes with an increase of the reaction line-force P' by the same factor β, if the force-input of the pendulum follows the coupling-pattern described by the DQEA; for if the realistic assumptions are made, that the pendulum acts like a rigid indenter and that the maximum penetration depth of the pendulum is small in comparison to the thickness of the specimen, then the angular distribution of the relative energy, emitted per time-interval into the tested specimens, can be considered as being approximately P-independent. Furthermore, if the central bar-channel remains nearly geometrically unchanged during the Charpy test until rupture occurs by unstable crack extension, then the proportionality between P and P' is evident. The mentioned assumptions are acceptable for ferritic-martensitic steels, which are tested in the DBTT-range. The same is evident for other materials at any testing-temperature, if their toughness potential is similar to the one of ferritic-martensitic steels being tested in the DBTT-range.

The short retardation-time of the reaction line-force P', which is built up at the notch-tip, with regard to the pendulum force P acting at the impact contact, has not yet been considered. However, this effect is thought to be negligible for common types of Charpy impact specimens for the following reasons: First, the impact contact zone is situated close to the process zone in this case [3]. Secondly, the time needed to transmit the reaction of an increase of the pendulum force P to the process zone at the notch tip by longitudinal stress waves is much smaller than the time-interval, which is marked by the begin of loading of the specimen and its start of final, brittle failure. Consequently, the error arising by assuming proportionality between P and P' is small with respect to the mentioned retardation effect, i.e. P is only changing very few during the short retardation-time of P', if the Charpy impact tests are performed with the usual pendulum speeds (1–5 m/s). In addition, the retardation-time is always the same for tests being performed with equal pendulum speeds. Thus, the error might be even considerably minor for Charpy impact tests, which are focused on the scatter of scaled maximum impact line-forces. The latter is

the claim for the evaluation method being developed later on in this article.

In order to be able to apply the DQEA, it must be avoided, that brittle failure already occurs in the inertia-affected load stage. On the contrary, a process zone and the corresponding residual stress field with compressive components has to be formed by localized, partially adiabatic, elasto-plastic deformation during the inertia-affected load stage. Hence, the testing-temperature must not be selected much lower than the DBTT, thus still enabling at least the formation of a minimum process zone due to adiabatic heating; for the minimum process zone hinders the tested specimen from undergoing brittle fracture already in the inertia-affected load stage. Besides, the formation of a process zone is a prerequisite for the occurrence of stable crack growth and, consequently, the possibility of using the DQEA. The DQEA then enables the evaluation of dynamic Weibull moduli m' from instrumented Charpy impact tests. The dynamic Weibull moduli m' are expected to be nearly testing-temperature-independent, if the tests are performed in the DBTT-range and if the DQEA is valid; for m' has only been evaluated from the lower $P_{\max}$-range of series of Charpy tests, being performed under equal testing conditions. Thus, m' is merely related to the testing-temperature-independent, brittle cleavage fracture events starting from minimum process zones, which occur in the whole DBTT-range although with temperature-dependent frequencies.

3. Localized deformation and residual stress fields

In the case of dynamic Charpy impact testing of brittle materials, undergoing stable crack growth prior to failure, only the stress distribution in the process zone along the notch-tip of the specimen is relevant; for the formation of maximum tensile stresses, as well as nucleation and growth of cracks and microcracks, take place in this area. Therefore, dynamic Charpy impact tests with materials, which fulfill the conditions mentioned in Section 2, can be modelled in the framework of the DQEA by three-point bend tests being overlaped by simultaneously performed static indentation tests. The static indentation tests provide the local reaction line-force P' along the notch-tip, and the simultaneously performed three-point bend tests, give rise to the additional relevant normal stresses in the central bar-channel along the mid-plane [6]. Besides, the relevant normal stress in the small process zone has been approached in the framework of the DQEA, by the approximately uniform value σ (see Fig. 1). Differences between the predicted stress distributions of the DQEA and the real stress distributions of the corresponding Charpy impact tests are thus restricted to the remaining side-parts of the specimen. On the other side, it has already been shown in Section 2, that the stress distribution outside the process zone is irrelevant for the considered type of Charpy impact testing in the DBTT-range.

Cook and Clarke [10] developed a two-component model, which can be applied to situations, being characterized by stable crack growth under the influence of both an uniform applied stress and a local contact load, the latter being equivalent to a local, residual stress field [6, 8, 10]. As a matter of fact, it is possible to assign the uniform applied stress to the normal stress σ, if the process zone of a Charpy specimen is considered, whereas the local contact load can be assigned in this case to the reaction line-force P' acting at the notch-tip and producing the local residual stress field being related to the process zone. Consequently, the Cook-and-Clarke model (CCM) is also valid for three-point bend tests being overlaped by simultaneously performed static indentation tests at the notch-tip, i.e. the CCM can be used for the evaluation of data of instrumented Charpy impact tests, if the DQEA is valid.

Cook and Clarke [10] modelled the driving force for fracture as the sum of two components, one stabilizing and the other destabilizing crack propagation. Thus, the net stress intensity factor K_I is also consisting of two components. The first component K_{a} arises from the uniform applied stress σ destabilizing crack propagation, and the second component K_{r} is due to a localized loading F decreasing the driving force for fracture with increasing crack length c. The localized component is modelled as a residual stress intensity factor, arising from the elastic-plastic deformation field of a sharp particle contact. The resistance to crack extension, the R-curve, has been described in this two-component model by an increasing power law $R \propto c^{2\tau}$ (the toughening exponent τ is characterizing the rate of toughness increase with increasing crack length). Besides, the following restriction $0 \leq \tau \leq 0.5$ is valid, because, otherwise, no stable crack growth can occur in the framework of the CCM [10].

Using equilibrium fracture criteria, it is possible to describe the fracture behaviour of brittle materials undergoing an amount of stable crack growth prior to failure, in terms of applied stress, localized loading and crack length. The following calculations are mainly based on the original treatment of Cook and Clarke [10]. The net stress intensity K_I is given in the two-component model by

$$K_I = K_{\mathrm{a}} + K_{\mathrm{r}} \tag{12}$$

According to Linear Elastic Fracture Mechanics (LEFM) the applied stress intensity factor K_{a} always takes the form [11]

$$K_{\mathrm{a}} = d_1 \sigma \sqrt{c} \tag{13}$$

Furthermore, the constants are denoted by d_1, $d_2, \ldots, d_i$. The local component K_{r} represents the residual stress intensity factor arising from a localized, elastic/plastic deformation field [10]. K_{r} might be the result of a sharp particle contact or of other interaction mechanisms, however, it is mostly possible to treat it with the following equation [6, 10],

$$K_{\mathrm{r}} = d_2 F c^{-\frac{r}{2}} \tag{14}$$

whereby r denotes a numerical constant characterizing the geometry of the localized loading. The fracture

resistance, and hence the toughness T, is related to the work necessary for incremental crack extension R by

$$T = \sqrt{RE} \tag{15}$$

whereby E denotes the Young's modulus [10, 11]. On the other side, the R-curve is usually assumed to show the power law dependence $R \propto c^{2\tau}$ [6, 10, 11]. Thus, we find for the fracture toughness T:

$$T = d_3 c^{\tau} \tag{16}$$

An equilibrium for the fracture system has been obtained, only when the mechanical energy released for a virtual crack advance equals the work used to create new crack surfaces. In terms of stress intensity factor K_I and toughness T, the equilibrium condition facilitating stable crack propagation is simply defined by $K_I = T$. According to Equations 12–16 the equilibrium condition can thus be written as follows:

$$d_1 \sigma \sqrt{c} + d_2 F c^{-\frac{r}{2}} = d_3 c^{\tau} \tag{17}$$

In the framework of the DQEA, this equilibrium condition is thought to be fulfilled locally in the process zone of the Charpy specimen. Moreover, the instability condition, which is characterizing the begin of brittle failure by unstable crack propagation, is also assumed to be valid in this case, at least in the process zone, if the DQEA is valid. The instability condition is given by [10],

$$\frac{\partial K_I}{\partial c} = \frac{1}{2} d_1 \sigma_f c_f^{-\frac{1}{2}} - \frac{r}{2} d_2 F_f c_f^{-\frac{r}{2}-1} = \tau d_3 c_f^{\tau-1} = \frac{\partial T}{\partial c} \tag{18}$$

whereby the variables σ_f, F_f and c_f are special cases of σ, F and c refering to the uniform stress, localized load and crack length values, which correspond to the onset of unstable crack propagation, i.e. brittle failure. Therefore, Equations 12–17 are also true if σ, F and c are replaced by σ_f, F_f and c_f. In the framework of the DQEA, being focussed on the process zone of the specimens, the maximum normal stress σ_{max}, arising in the process zone, is considered to be equivalent to the uniform applied stress σ_f of the CCM, and the maximum reaction line-force P'_{max}, arising during the Charpy impact test prior to brittle failure, can be regarded as being equivalent to the localized loading F_f of the CCM. However, the meaning of the crack length remains unaltered. If c and c_f are eliminated in equations 17 and 18, the following relation is found [6, 10]:

$$\sigma = d_4 (P'_{max})^{\frac{2\tau-1}{2\tau+r}} \tag{19}$$

Finally, the numerical constant r is equal to one for a line-force center loading of a linear crack [10]. This is the case for the reaction line-force P', acting on the process zone along notch-tip of the Charpy specimens (see Fig. 1). The process zone is always the nucleation site of the critical, linear crack, which undergoes an amount of stable crack growth prior to become unstable and promote brittle failure. The impact line-force P, which is directly measured by performing instrumented Charpy impact tests, is assumed to be proportional to P' according to the DQEA. Thus, we find

$$\sigma \propto (P_{max})^{\frac{2\tau-1}{2\tau+1}} \tag{20}$$

whereby P_{max} denotes the maximum impact line-force arising during Charpy impact tests, if the DQEA applies.

4. Dynamic Weibull master curves

According to Equation 20 of Section 3, it is possible to express the cumulative Weibull failure probability distribution $P(\sigma)$ also in terms of the maximum impact line-force P_{max}, if the threshold load-value $P_{max\,\tau}$, below which the cumulative probability of failure would be 100%, is equal to zero [6, 10];

$$P(P_{max}) = 1 - \exp\left[-\left(\frac{P_{max}}{P_{max\,0}}\right)^{m'}\right] \tag{21}$$

whereby m' denotes a modified, dynamic Weibull modulus defined by

$$m' = m\frac{2\tau - 1}{2\tau + 1} \tag{22}$$

$P_{max\,0}$ represents a normalizing factor which has dimensions of load. The approach $P_{max\,\tau} \approx 0$ is plausible especially for materials undergoing an amount of stable crack growth prior to failure; for in these cases no significant thresholds are probable, which do not result at least in microstructural changes. Microstructural changes, however, are already taken into account by appropriately defined deviation parameters characterizing the toughening potential of the investigated material. Thus, the introduction of a threshold load $P_{max\,\tau}$ is not necessary in these cases. Besides, m' is always negative, because the following limitation for the toughening exponent τ is valid [10]: $0 \leq \tau \leq 0.5$. Consequently, $P(P_{max} = 0)$ is equal to one, although in the quasi-static case $P(\sigma = 0)$ is equal to zero.

The dynamic Weibull master curves $M[e'(z), m']$, $I(x', m')$ and $K(y', m')$, are derived from the two-parameter cumulative failure probability distribution function $P(P_{max})$ in the same way, as the quasi-static Weibull master curves $M[e(z), m]$, $I(x, m)$ and $K(y, m)$ have been derived from the three-parameter cumulative failure probability distribution function $P(\sigma)$ [4]. The scaled, dynamic variables $e'(z)$, x' and y' have been defined like the scaled, quasi-static variables $e(z)$, x and y; however, the role of the applied failure stress σ is played in the dynamic case by the maximum impact line-force P_{max}. Moreover, the quasi-static parameters σ_z, σ_{in}, σ_o, σ_i and $\bar{\sigma}$ correspond to the dynamic parameters $P_{max\,z}$, $P_{max\,in}$, $P_{max\,0}$, P_{max_i} and $\bar{P}_{max}$, whereas the quasi-static threshold parameter σ_τ corresponds to zero in the dynamic case. Under dynamic loading conditions, being related to negative, dynamic Weibull moduli $m' < 0$, experimental failure data $(P_{max_i};\ P(P_{max_i}))$ are evaluated with the help of a step function $H'[e'(z)]$;

this function has been defined as being equal to one for $e'(z) < e'_{cr}$ and equal to zero for $e'(z) \geq e'_{cr}$; e'_{cr} is representing the $e'(z)$-value corresponding to the cross-over point of the experimental dynamic Weibull master curve $M\exp[e'(z), m']$ and the corresponding theoretical dynamic Weibull master curve $M[e'(z), m']$. The two areas being formed between the step function $H'[e'(z), m']$ and $M[e'(z), m']$, are denoted by $FiM1'[e'(z)]$ and $FiM2'[e'(z)]$. $F\exp 1M'[e'(z)]$ and $F\exp 2M'[e'(z)]$ represent the two areas formed between $M\exp[e'(z), m']$ and $M[e'(z), m']$, whereby $M\exp[e'(z), m']$ is constructed by calculating the dynamic Weibull modulus m' from the lower P_{max}-range of the experimental, cumulative failure probability distributions $P(P_{max_i})$ [4–6]. Besides, $FiM1'[e'(z)]$ and $F\exp 1M'[e'(z)]$ represent the areas being situated below the cross-over point $e'_{cr}(z)$, whereas the opposite is valid for $FiM2'[e'(z)]$ and $F\exp 2M'[e'(z)]$. With the help of $FiM1'[e'(z)]$, $FiM2'[e'(z)]$, $F\exp 1M'[e'(z)]$ and $F\exp 2M'[e'(z)]$ significant quotients, characterizing the dynamic toughening potential of the investigated materials, can be defined. The dynamic, material-specific quotients $d\chi_M$, $d\chi_I$ and $d\chi_k$ are defined in analogy to the quasi-static, material-specific quotients χ_M, χ_I and χ_k [5].

$$d\chi_M = \frac{FiM1'[e'(z)]/FiM2'[e'(z)]}{F\exp 1M'[e'(z)]/F\exp 2M'[e'(z)]} \quad (23)$$

The $d\chi_M$-values of the special dynamic master curves $I(x', m')$ and $K(y', m')$, denoted by $d\chi_I$ and $d\chi_k$, are easily calculated by strictly replacing z by z_{in} or $\overline{z}$ in all relevant formulas, which are related to the general type of Weibull master curves $M[e'(z), m']$ and $M\exp[e'(z), m']$.

$$d\chi_I = \frac{FiM1'[e'(z_{in})]/FiM2'[e'(z_{in})]}{F\exp 1M'[e'(z_{in})]/F\exp 2M'[e'(z_{in})]} \quad (24)$$

$$d\chi_k = \frac{FiM1'[e'(\overline{z})]/FiM2'[e'(\overline{z})]}{F\exp 1M'[e'(\overline{z})]/F\exp 2M'[e'(\overline{z})]} \quad (25)$$

The dynamic quotients $d\chi_M$, $d\chi_I$ and $d\chi_k$, being related to negative dynamic Weibull moduli m', are expected to come out as material-specific, in a first approach, like the quasi-static quotients χ_M, χ_I and χ_k [5]. $d\chi_M$, $d\chi_I$ and $d\chi_k$ are positive and finite for $m' < -1$. Unfortunately, these dynamic quotients are not helpful for $-1 < m' < 0$; for $d\chi_M$ and $d\chi_I$ are constantly zero in these cases, since the corresponding deviation parameters $FiM2'[e'(z)]$ and $FiM2'[e'(z_{in})]$ exhibit positive-infinite values, whereas $d\chi_k$ is not even always existing as a real number for this restricted m'-range. The dynamic master curves $M[e'(z = 0.5), m']$ and $I(x', m')$ are displayed in Figs 2 and 3 for $m' < 0$, whereas the master curves $K(y', m')$ are depicted in Fig. 4 for $m' < -1$. The transformation equations for the three types of quasi-static master curves, which have already been given in part 1 of this series of papers by Equations 9–15 and 37–43 [4], are also true for the dynamic Weibull master curves.

If the different types of dynamic Weibull master curves are compared to one another at distinct values of the scaled variables by setting $e'(z = 0.5) = x' = y' =$ constant, the following relation is found to be valid for $m' < 0$:

$$I(x', m') > 1 - \frac{1}{e} \approx 0.63 > M[e'(z = 0.5), m'] = 0.5 \quad (26)$$

In addition, for experimentally relevant, dynamic Weibull moduli $-1 > m' > \approx -10^8$ the following relation has been verified:

$$I(x', m') > M[e'(z = 0.5), m'] > K(y', m') \quad (27)$$

The general dynamic deviation parameters $FiM1'[e'(z)]$, $FiM2'[e'(z)]$, $F\exp 1M'[e'(z)]$ and $F\exp 2M'[e'(z)]$ can be defined analytically as follows:

$$FiM1'[e'(z)] = \int_0^{e'_{cr}(z)} \{1 - M[e'(z), m']\}\, d[e'(z)] \quad (28)$$

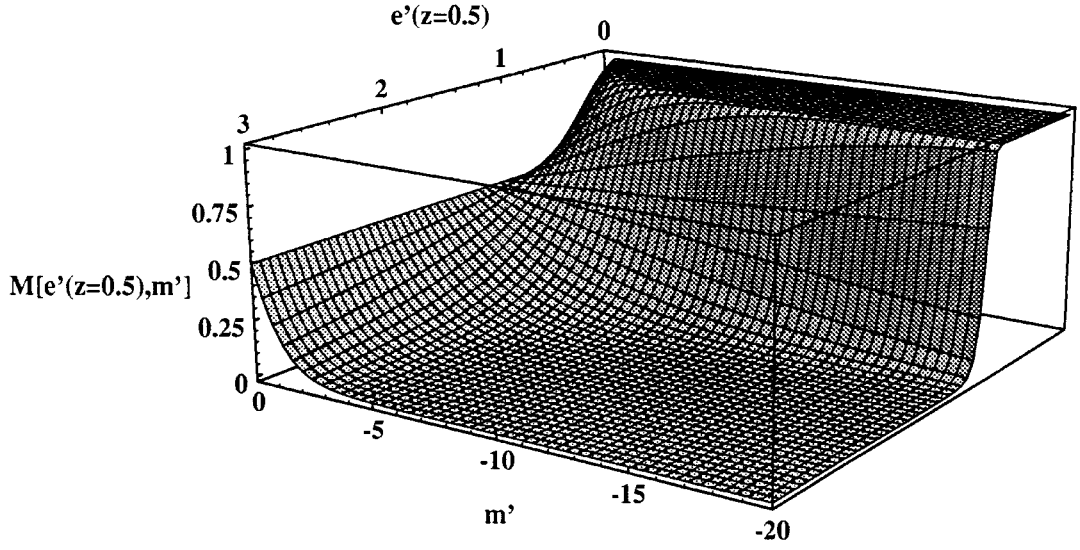

Figure 2 The general type of dynamic Weibull master curves $M[e'(z = 0.5), m']$ being related to the cumulative failure probability $z = 0.5$.

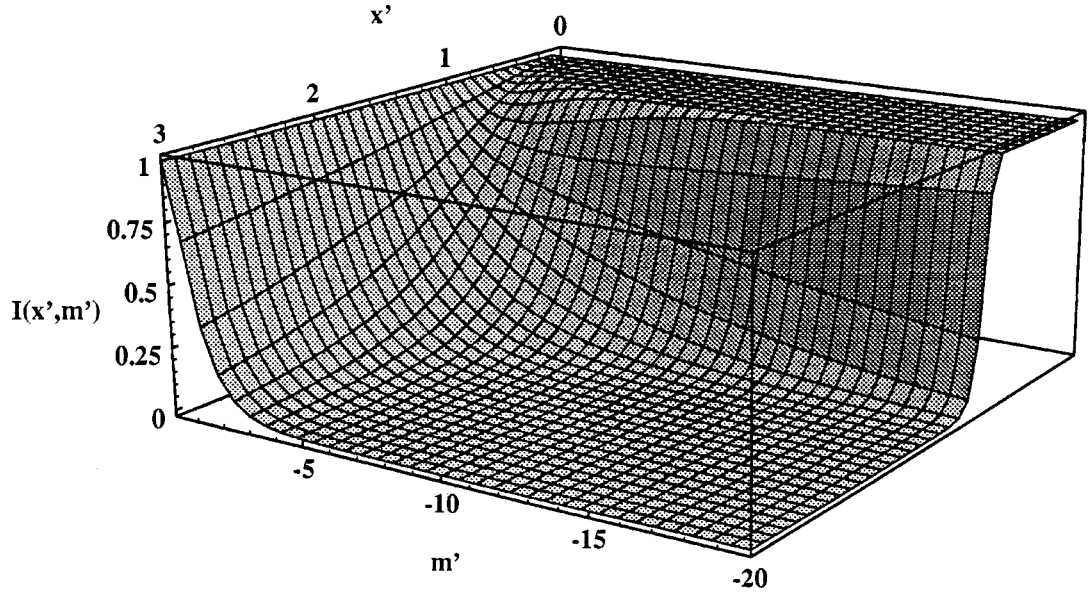

Figure 3 The special type of dynamic Weibull master curves $I(x', m')$.

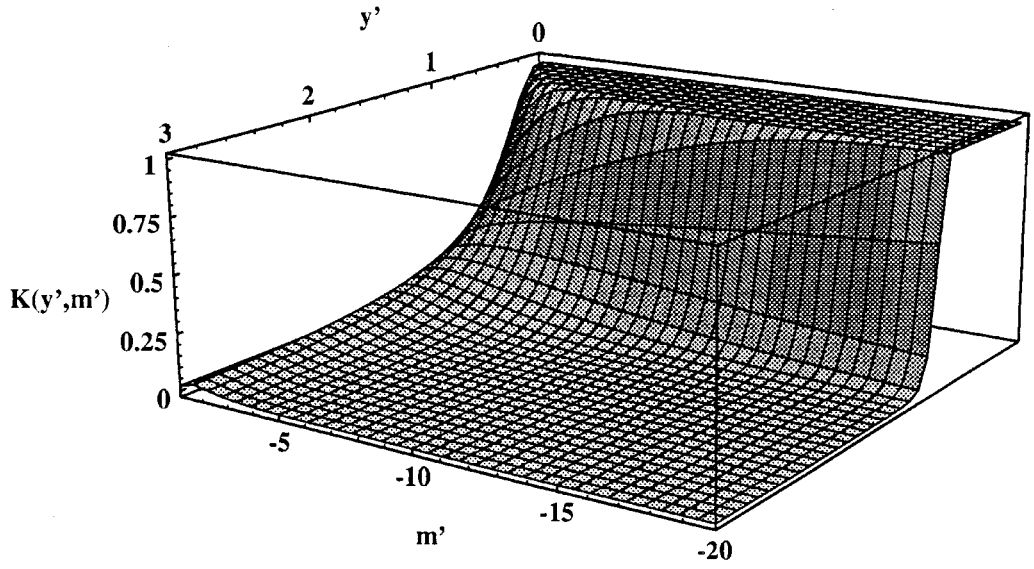

Figure 4 The special type of dynamic Weibull master curves $K(y', m')$.

$$FiM2'[e'(z)] = \int_{e'_{cr}(z)}^{\infty} \{M[e'(z), m']\}\, d[e'(z)] \quad (29)$$

$$F\exp 1M'[e'(z)] = \int_{0}^{e'_{cr}(z)} |M\exp[e'(z), m'] - M[e'(z), m']|\, d[e'(z)] \quad (30)$$

$$F\exp 2M'[e'(z)] = \int_{e'_{cr}(z)}^{\infty} |M\exp[e'(z), m'] - M[e'(z), m']| d[e'(z)] \quad (31)$$

The dynamic deviation parameters of the special master curves $I(x', m')$ and $K(y', m')$ are obtained, if z is replaced by z_{in} or $\overline{z}$ in Equations 28–31.

$$\begin{aligned} FiM1'[e'(z_{in})] &= \int_{0}^{e'_{cr}(z_{in})} \{1 - M[e'(z_{in}), m']\}\, d[e'(z_{in})] \\ &= \int_{0}^{x'_{cr}} [1 - I(x', m')]\, dx' \end{aligned} \quad (32)$$

$$\begin{aligned} FiM2'[e'(z_{in})] &= \int_{e'_{cr}(z_{in})}^{\infty} \{M[e'(z_{in}), m']\}\, d[e'(z_{in})] \\ &= \int_{x'_{cr}}^{\infty} I(x', m')\, dx' \end{aligned} \quad (33)$$

$$F\exp 1M'[e'(z_{\text{in}})] = \int_0^{e'_{\text{cr}}(z_{\text{in}})} |M\exp[e'(z_{\text{in}}), m'] - M[e'(z_{\text{in}}), m']|\, d[e'(z_{\text{in}})]$$
$$= \int_0^{x'_{\text{cr}}} |I\exp(x', m') - I(x', m')|\, dx' \qquad (34)$$

$$F\exp 2M'[e'(z_{\text{in}})] = \int_{e'_{\text{cr}}(z_{\text{in}})}^{\infty} |M\exp[e'(z_{\text{in}}), m'] - M[e'(z_{\text{in}}), m']|\, d[e'(z_{\text{in}})]$$
$$= \int_{x'_{\text{cr}}}^{\infty} |I\exp(x', m') - I(x', m')|\, dx' \qquad (35)$$

$$FiM1'[e'(\bar{z})] = \int_0^{e'_{\text{cr}}(\bar{z})} \{1 - M[e'(\bar{z}), m']\}\, d[e'(\bar{z})]$$
$$= \int_0^{y'_{\text{cr}}} [1 - K(y', m')]\, dy' \qquad (36)$$

$$FiM2'[e'(\bar{z})] = \int_{e'_{\text{cr}}(\bar{z})}^{\infty} \{M[e'(\bar{z}), m']\}\, d[e'(\bar{z})]$$
$$= \int_{y'_{\text{cr}}}^{\infty} K(y', m')\, dy' \qquad (37)$$

$$F\exp 1M'[e'(\bar{z})] = \int_0^{e'_{\text{cr}}(\bar{z})} |M\exp[e'(\bar{z}), m'] - M[e'(\bar{z}), m']|\, d[e'(\bar{z})]$$
$$= \int_0^{y'_{\text{cr}}} |K\exp(y', m') - K(y', m')|\, dy' \qquad (38)$$

$$F\exp 2M'[e'(\bar{z})] = \int_{e'_{\text{cr}}(\bar{z})}^{\infty} |M\exp[e'(\bar{z}), m'] - M[e'(\bar{z}), m']|\, d[e'(\bar{z})]$$
$$= \int_{y'_{\text{cr}}}^{\infty} |K\exp(y', m') - K(y', m')|\, dy' \qquad (39)$$

5. Discussion and conclusions

According to the DQEA, an indirect correspondence exists between the dynamic maximum impact line-force $P_{\max}$ and the quasi-static applied failure stress σ, i.e. high applied failure stresses in quasi-static tests correspond to low maximum impact line-forces in dynamic tests. This fact is the consequence of the quasi-static Weibull moduli m being positive, as well as the dynamic Weibull moduli m', which always exhibit negative values. The interpretation of the dynamic deviation parameters with respect to the CCM will mainly be performed for the general type of dynamic Weibull master curves $M[e'(z), m']$ of ferritic-martensitic steels in part 4 of this series of papers. Nevertheless, the evaluated consequences will also be true for the two other types of dynamic Weibull master curves $I(x', m')$ and $K(y', m')$, since they represent special cases of $M[e'(z), m']$ being displayed in specific notations.

The dynamic Weibull master curves $I(x', m')$ and $I\exp(x', m')$, as well as the dynamic deviation parameters $FiM1'[e'(z_{\text{in}})]$, $FiM2'[e'(z_{\text{in}})]$, $F\exp 1M'[e'(z_{\text{in}})]$, $F\exp 2M'[e'(z_{\text{in}})]$ and $d\chi_I$, are the most convenient means for the evaluation of Charpy impact tests; for these Weibull master curves show a favorable value-distribution in the relevant m'-range according to Equations 26–27, and they can be obtained for all the possible dynamic Weibull moduli $m' < 0$. Moreover, they are related to a scaling factor, which is experimentally highly relevant being the most probable maximum impact line-force $P_{\max\text{in}}$. Finally, $K(y', m')$, $K\exp(y', m')$, $M[e'(z), m']$ and $M\exp[e'(z), m']$ can usually be calculated from $I(x', m')$ and $I\exp(x', m')$ by using the transformation equations given in part 1 of this series of papers [4] being valid for experimental as well as theoretical quasi-static and dynamic Weibull master curves.

References

1. R. L. KLUEH, K. EHRLICH and F. ABE, *J. Nucl. Mater.* **191** (1992) 116.
2. N. S. CANNON and D. S. GELLES, *ibid.* **186** (1991) 68.
3. K. KROMPHOLZ, P. TIPPING and G. ULLRICH, *Z. Werkstofftech.* **15** (1984) 199.
4. M. LAMBRIGGER, part 1 of this series of papers, *J. Mater. Sci.* to be published.
5. *Idem.*, part 2 of this series of papers, *ibid.* to be published.
6. *Idem., J. Mater. Sci. Lett.* **16** (1997) 298.
7. *Idem., ibid.* **16** (1997) 924.
8. *Idem., Phil. Mag.* **A77** (1998) 363.
9. C. H. NGUYEN, in Proceedings of the 11th Biennial European Conference on Fracture, 3–6 September 1996, edited by J. Petit, J. de Fouquet, G. Henaff, P. Villechaise and A. Dragon (Engineering Materials Advisory Services Ltd., Warley 1996) Vol. 1, p. 687.
10. R. F. COOK and D. R. CLARKE, *Acta Metall.* **36** (1988) 555.
11. D. BROOK, in "Elementary Engineering Fracture Mechanics" (Martinus Nijhoff Publishers, Dordrecht, 1987) p. 10.

Received 22 September 1998
and accepted 2 March 1999